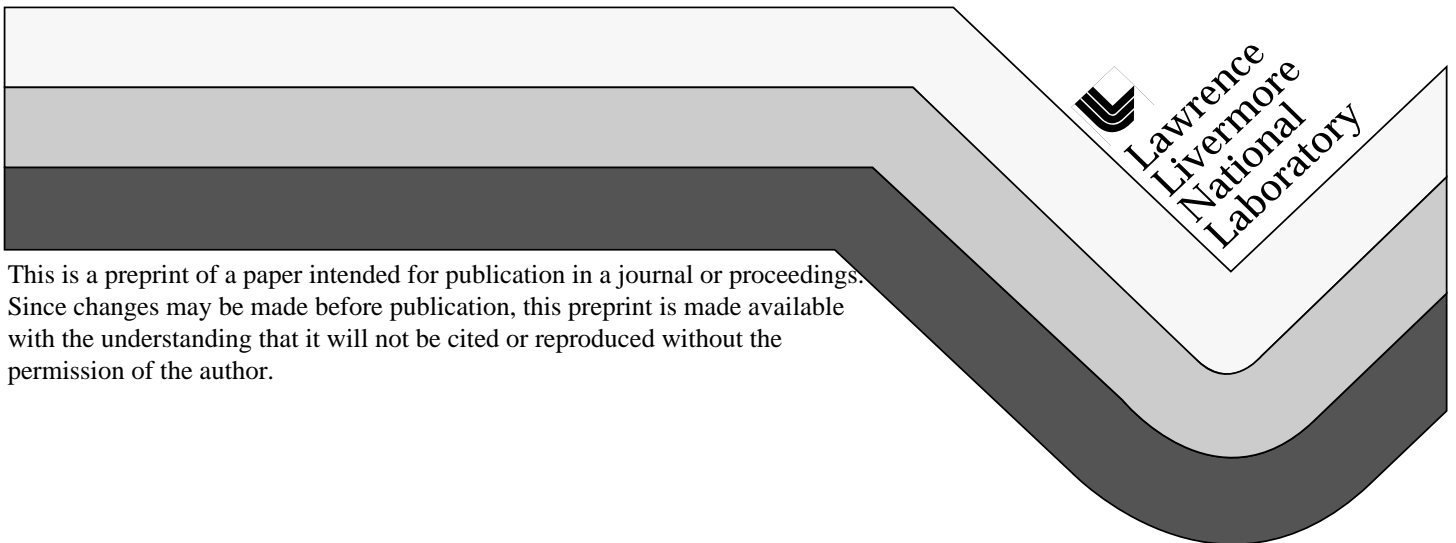


Three-Degree-of-Freedom Optic Mount for Extreme Ultraviolet Lighthography

H. Tajbakhsh, L. Hale, T. Malsbury,
S. Jensen and J. Parker

This paper was prepared for submittal to
American Society for Precision Engineering 13th Annual Meeting
St. Louis, MO
October 25-30, 1998

August 27, 1998



DISCLAIMER

This document was prepared as an account of work sponsored by an agency of the United States Government. Neither the United States Government nor the University of California nor any of their employees, makes any warranty, express or implied, or assumes any legal liability or responsibility for the accuracy, completeness, or usefulness of any information, apparatus, product, or process disclosed, or represents that its use would not infringe privately owned rights. Reference herein to any specific commercial product, process, or service by trade name, trademark, manufacturer, or otherwise, does not necessarily constitute or imply its endorsement, recommendation, or favoring by the United States Government or the University of California. The views and opinions of authors expressed herein do not necessarily state or reflect those of the United States Government or the University of California, and shall not be used for advertising or product endorsement purposes.

Three-Degree-of-Freedom Optic Mount for Extreme Ultraviolet Lithography

H. Tajbakhsh, L. Hale, T. Malsbury, S. Jensen, J. Parker
Lawrence Livermore National Laboratory
Livermore, CA 94550

Abstract

A mechanism to finely align optics for extreme ultraviolet lithography applications is presented. The mechanism is a small motion parallel link manipulator with flexure joints that exhibits nanometer level positioning capability. Performance results of a prototype system are given in this paper.

Keywords: precision stage, flexure, kinematic design, parallel link manipulator, error budget, thermal stability, EUVL

Introduction

The projection optics required for extreme ultraviolet lithography (EUVL) must be precisely figured to sub-nanometer rms surface figure accuracy over 50 to 150 mm apertures and multi-layer coated for high reflectivity. This requires extending the state of the art in optics manufacturing, multi-layer coatings and optics metrology. Accordingly, the opto-mechanical system design must represent a small proportion of the total figure error budget. In addition, final alignment of optics in the projection optics system requires motorized adjustments with nanometer-level resolution, sub-millimeter range, and a high degree of dimensional stability. A prototype actuation system meeting these requirements has been built.

The information required to calculate the desired mirror positions comes from interferometric measurements of the assembled optical system's wavefront over multiple field points. The typical optic requires motorized adjustments in three degrees of freedom, namely, translation along the optical axis (piston) and rotation about the two axes in the plane of the optic (tip and tilt). Once aligned, the actuation system is disabled until realignment is required at some future date. The actuation system is not presently intended to provide real-time imaging system compensation during EUV lithography operation. This paper presents our design solution for the actuated three-degree-of-freedom optic mount. The discussion includes system design issues, error budget analyses related to satisfying long-term and short-term dimensional stability, and experimental results from a prototype system.

System Design

System design requirements for the actuation system flow down from the optical design and stability

requirements for a scanning lithographic machine. The resolution requirement for actuation is less than 10 nm in translation and less than 30 nrad in rotation. Furthermore, the system must demonstrate long-term dimensional stability, high dynamic stiffness, and have little effect on the optic's surface figure when actuated to its limits of motion (± 100 microns).

A parallel mechanism allowing translation at three points around the periphery of the optic cell is chosen to meet these requirements. Monolithic flexures provide friction-free joint movement and superior temporal dimensional stability. This particular actuation system uses three identical flexure mechanisms that transmit radial motion from high-resolution piezo screws to a 5:1 reduced axial motion at the cell's periphery. Simultaneous and equal motion of the three piezo screws provides pure axial translation of the cell (piston) while differential motion of the motors provides rotation of the optic cell (tip and tilt).

The piezo screws have a resolution generally less than 30 nm and with the 5:1 transmission ratio provide the required resolution. Capacitance sensors located on the optic cell near the three-actuation positions provide feedback for the optic cell movements. Capacitance sensors have subnanometer resolution with low thermal and electrical drift characteristics. The system without the capacitance gauges is shown in Figure 1.

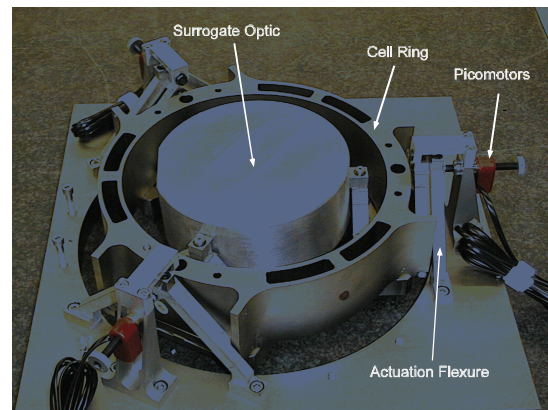


Figure 1: Prototype Actuation System

The optic cell that holds the optic is actuated in three degrees of freedom by actuation flexures that are located 120 degrees apart around its perimeter. Each actuation flexure is electrodischarge machined (EDM) from a single piece of Super Invar to maximize dimensional stability. The monolithic flexure has two

functional parts, described as the transmission flexure and the constraint flexure, as shown in Figure 2.

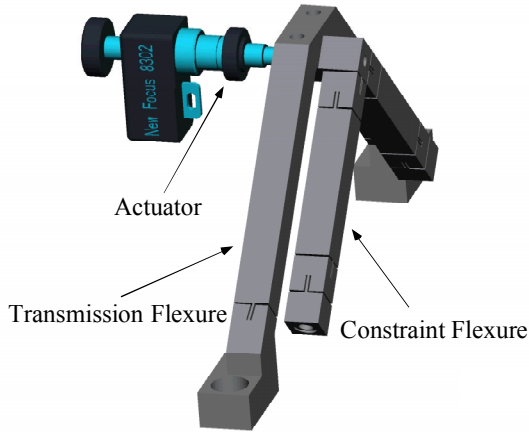


Figure 2: Detail of a single actuation flexure

The side of the actuation flexure that attaches to the projection optics housing is called the transmission flexure. The blades on this flexure form a hinge axis near their base so that movement of the piezo screw causes rotation of the transmission flexure about this axis. The role of the constraint flexure is to kinematically locate the optic cell with respect to the transmission flexure in two degrees of freedom. The plane of the blades in the transmission flexure intersects the instantaneous center of rotation of the constraint flexure. This condition maximizes the stiffness in the two constraint directions. Since the constraint flexure is offset from the transmission flexure, rotation of the transmission flexure produces displacement of the cell in the plane of the constraint flexure. Motion at the piezo screw is accommodated by compliance in the constraint flexure. This compliance also serves to isolate the optic cell from actuation related loads that could cause changes in the optical substrate figure.

Error Budget

An error budget provides a mechanism with which to evaluate tradeoffs in design and to predict overall system performance. The EUVL projection optics system is dominated by two basic sets of performance requirements. The first requirement is preservation of surface figure of the optics and the second is stability of the dimensional relationship between the optic surfaces. The total surface figure error budget is less than 0.25 nm rms over the clear apertures of the optics. Surface figure error is defined as the figure error between spatial frequency limits from the clear aperture to one inverse millimeter. Of the many contributors to the figure error budget, the actuation flexure contribution is set at less than 0.08 nm rms. Essentially, the actuation system can not influence the figure of the optics.

The dimensional stability requirement is broken down into scanning stability and long-term stability. The scanning requirement corresponds to a time scale related to that required for a single image scan. For the prototype EUVL system this is limited to approximately 10 seconds. Vibration is the primary error source related to this requirement. The long-term requirement is derived from the desire for an aligned imaging system to stay aligned within the operational environment for long periods of time. Thermal effects during operation and temporal dimensional changes of systems are the main issues affecting long term stability. A time scale ranging from many months to a year is chosen for this error budget. Effectively, the time scale sets the period after which major imaging system realignments must be performed. The dimensional stability requirements for each optical element for scanning and long term are given in Table 1. Long term stability of the joints, materials, and piezo screw in the actuation system are the topics of ongoing tests.

DOF	Scanning Error (rms)	Long Term Error
θ_x	3 nrad	$\pm 0.50 \mu\text{rad}$
θ_y	3 nrad	$\pm 0.50 \mu\text{rad}$
X	1 nm	$\pm 0.29 \mu\text{m}$
Y	1 nm	$\pm 0.29 \mu\text{m}$
Z	4 nm	$\pm 1.00 \mu\text{m}$

Table 1: Positioning Error Budget

Modal Analysis

A finite element modal analysis and experimental modal testing have been performed on the prototype actuation system. The finite element model (FEM) was constructed using shell and solid elements and the model was constrained similarly to the actual imaging system. The finite element analysis predicts the first mode of vibration to occur at 133 Hz. This is a longitudinal mode of vibration that is dominated by compliance in the actuation flexures.

The results of the experimental modal testing on the prototype actuation system agreed with the finite element model. The first dynamic mode occurred near 133 Hz as predicted by the FEM. The magnitude of the experimental frequency response function is shown in Figure 3. The range of the frequencies shown in Figure 3 is from 0 to 800 Hz.

A preliminary dynamic analysis using a low order representation of the EUVL projection optics system and the isolation systems has been completed. The results suggest that all structural modes of vibration should be greater than 150 Hz to ensure meeting the scanning stability goals. Based on these results, design changes have been implemented in the actuation system

that increase stiffness and raise the natural frequency to near 200 Hz. This was accomplished by adding structural reinforcement between the legs of the transmission flexures and increasing the blade width at the base of the flexures. Furthermore, increasing the blade thickness on the blades closest to the instant center increased the axial stiffness of the constraint flexures.

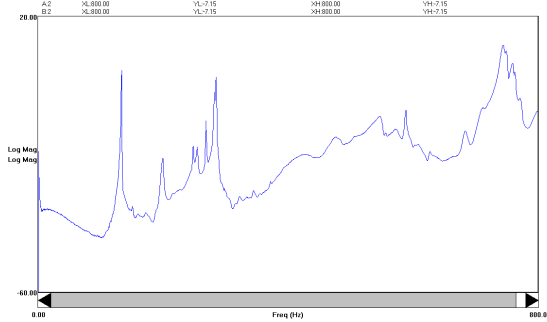


Figure 3: Frequency Response Function

Kinematics & Controls

The kinematics of this system can be modeled similar to traditional parallel link mechanisms such as the Stewart Platform Manipulator. For small amounts of z motion, the flexures can be kinematically modeled in terms of spherical, revolute and prismatic joints as shown in Figure 4.

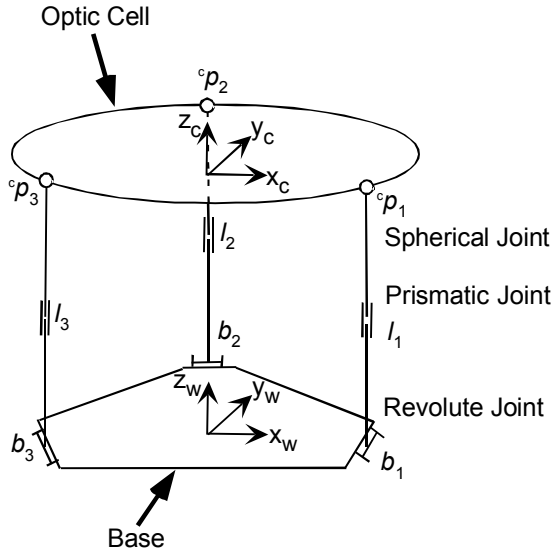


Figure 4: Kinematic Links and Parameters of the Actuation System

Mobility analysis shows that the system has three degrees of freedom as expected:

$$M = 6(m - j - 1) + \quad DOF = 6(8 - 9 - 1) + 15 = 3$$

where m is the number of members (8), j is the number of joints (9) and DOF is the total degrees of freedom of

the joints ($15=3*3+3*1+3*1$). The chosen degrees of freedom are rotations about x and y , and displacement in z , all occurring about the local coordinate system as defined by the chief ray point (point C) of the optic. This coordinate system is shown in Figure 4. The spatial coordinates of the base points (b_1, b_2, b_3) are defined in the world coordinate system (W), and the spatial coordinates of the platform points (p_1, p_2, p_3) are defined in the chief ray coordinate system (C).

The length of the prismatic joints can be written as:

$$l_1 = \sqrt{\left(T^? p_1 + d - b_1 \right) \left(T^? p_1 + d - b_1 \right)}$$

$$l_2 = \sqrt{\left(T^? p_2 + d - b_2 \right) \left(T^? p_2 + d - b_2 \right)}$$

$$l_3 = \sqrt{\left(T^? p_3 + d - b_3 \right) \left(T^? p_3 + d - b_3 \right)}$$

where T is the RPY (roll, pitch, and yaw) rotation matrix about z_c , y_c , and x_c , and d is the location of the C coordinate system relative to the W coordinate system. Note that the rotation about z (roll) is zero.

$$T = RPY(0, \theta, \psi) = \begin{bmatrix} \cos \theta & \sin \theta \sin \psi & \sin \theta \cos \psi \\ 0 & \cos \psi & -\sin \psi \\ -\sin \theta & \cos \theta \sin \psi & \cos \theta \end{bmatrix}$$

$$d = \begin{bmatrix} 0 & 0 & z \end{bmatrix}^T$$

These equations are used to direct the piezo screw displacement within a low bandwidth control scheme based on the capacitance gauge feedback. The graphical user interface of the controller receives user input as tip/tilt/piston motion about the chief ray point and computes the required movements in the joint space (l_1, l_2, l_3) using the kinematic equations. The control system drives the motors until the capacitance gauges reach their desired values.

Surface Distortion from Actuation System

To estimate the surface figure deformations due to actuation inputs from the piezo screws, detailed finite element models were created and analyzed using structural finite element model software. The optic is supported within the cell by three bipod mount flexures, similar to the previously mentioned constraint flexures. The collection of the three bipod mount flexures constrain the rigid body motion of the optical substrate, while partially isolating the substrate from disturbance forces and moments that deform the surface figure. The analyses considered the anticipated full range of motion of the optic, ± 100 microns in piston. Surface mesh plots of the clear aperture were generated using the extracted raw surface displacement data. For a 100 micron z displacement, the rms surface deformation is estimated to be 0.05 nm. Figure 5 shows an example of surface

deformations within the clear aperture boundary for an actuated optic with a nominal diameter and thickness of 170 mm and 65 mm respectively (clear aperture is 120 mm in diameter).

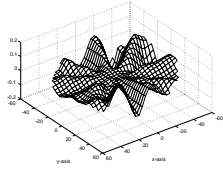


Figure 5: Mesh plot of surface deformations within the clear aperture (x,y: mm scale, z: nm scale)

Actuation Prototype Testing Results

The positioning capability of the actuation system was tested in a $\pm 0.5^\circ\text{C}$ temperature controlled environment. The positioning results for commanded Z motion are shown in Figure 6. The solid line shown in the figure represents the commanded motion and the dotted line is the actual position (capacitance gauge reading) of the actuated optic. The graph shows movement as small as 2 nm and as large as 50 nm. In simpler bench top testing, the system appears to demonstrate excellent dimensional stability, but the extreme demands of the EUVL imaging system require very exacting long-term measurements of dimensional stability. These tests are presently being initiated. Preliminary testing shows nanometer level stability for 0.5 minutes and longer in some cases. Ten-minute drift of all the capacitance gauges is shown in Figure 7. Thermal stability of 5 nm or less has been seen during this period.

To verify the commanded position, a displacement and angular measuring interferometer (He-Ne class II laser) is used to measure the commanded motion at the chief ray point. As configured, the interferometer has a 10 nm distance resolution and a $0.5 \mu\text{rad}$ angular resolution.

The effect of dead-air-path is reduced during the measurements by minimizing the distance between the mirrors and the interferometer. A small sample of the results from the testing of the positioning and angular displacements is given in Table 2. Motion about the unactuated axes is also measured during movement of controlled axes and the results are reported in Table 3.

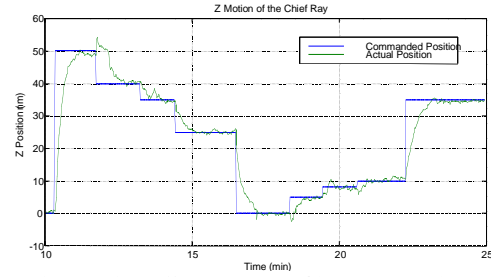


Figure 6: Z Commanded/Actual Motion Of the Chief Ray Point

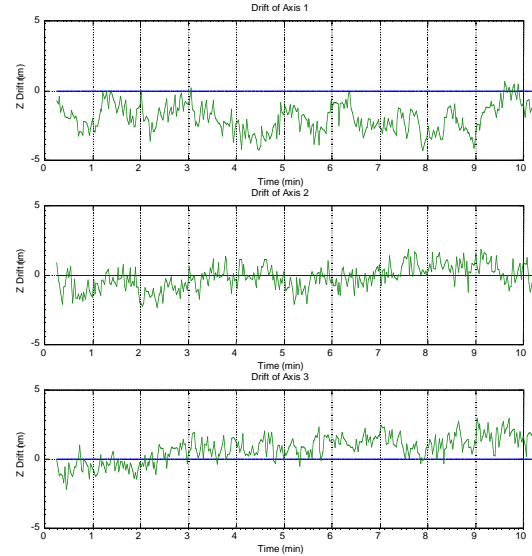


Figure 7: Short Term Capacitance Gauge Drift

Trial	Dir.	Commanded Position	Measured Position
1	Z	100 nm	$100 \pm 10^\dagger$ nm
2	θ_x	$5 \mu\text{rad}$	$4.84 \pm 0.484^\ddagger$ μrad
3	θ_y	$28 \mu\text{rad}$	$27.6 \pm 0.484^\ddagger$ μrad

† Resolution of the DMI

‡ Resolution of the AMI

Table 2: DMI/AMI Measurements

Trial	Commanded Axis	Measured Axis
1	Z=-100 nm	$X < 10^\dagger$ nm
2	$\theta_x = 5 \mu\text{rad}$	$X < 10^\dagger$ nm
3	$\theta_y = 5 \mu\text{rad}$	$X < 10^\dagger$ nm

† Resolution of the DMI

Table 3: Undesirable Motion Of the Actuation Cell

This work was performed under the auspices of the U. S. Department of Energy by the Lawrence Livermore National Laboratory under contract no. W-7405-Eng-48.